About a few Challenges for Signal Processing in emission and transmission tomography

Pr Christian MOREL
Centre de Physique des Particules de Marseille

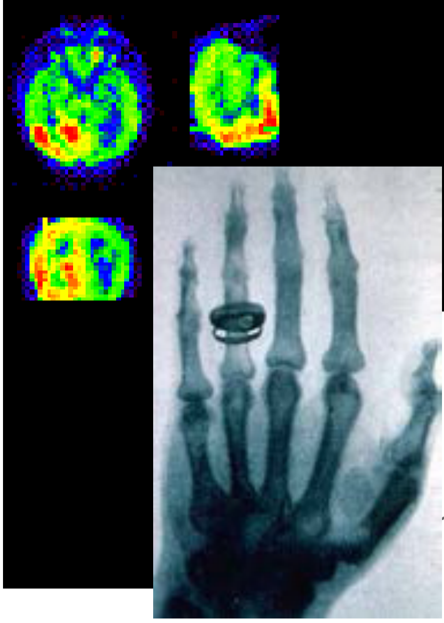

Tomography

From Greek *tomê* (slice)
+
graphô (write)
=
Representation into slices

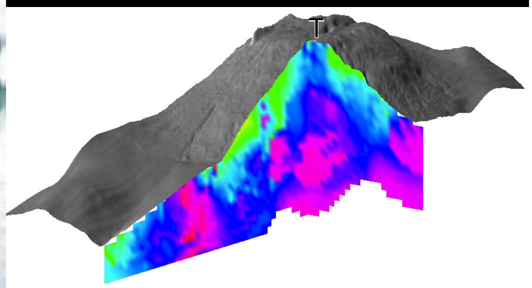

Signal Processing in Tomography – INFIERI – Paris – July 15 2014

Positron Emission Tomography (PET)

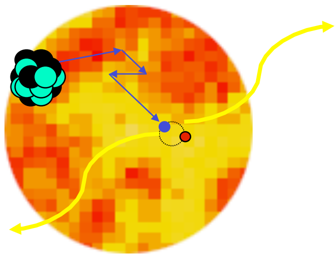

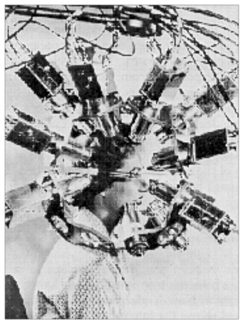

Wrenn et al. The use of positron emitting radioisotopes for the localization of brain tumours *Science* **113** (1951) 525

Signal Processing in Tomography – INFIERI – Paris – July 15 2014

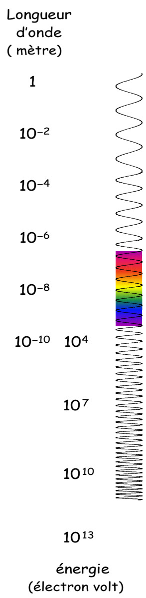

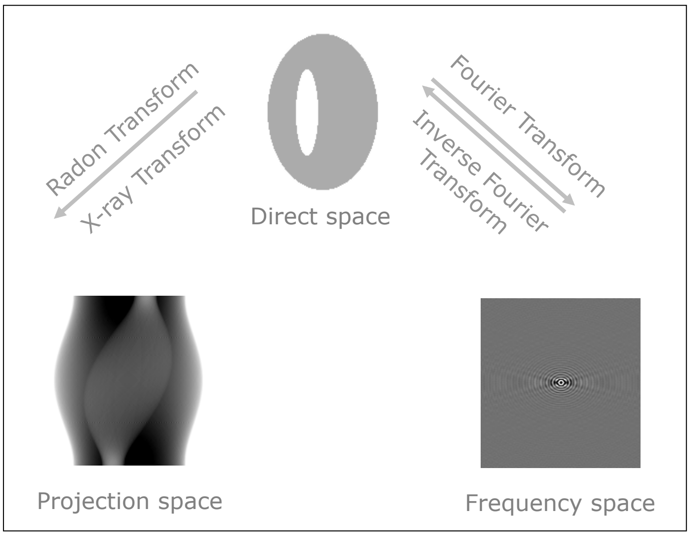

Signal Processing in Tomography – INFIERI – Paris – July 15 2014

Two dimensional image reconstruction

1963: Alan McLeod Cormack

Rediscovery of an analytical inversion already published by Radon en 1917 to reconstruct an object in two dimensions (2D) from its line integrals (projections)

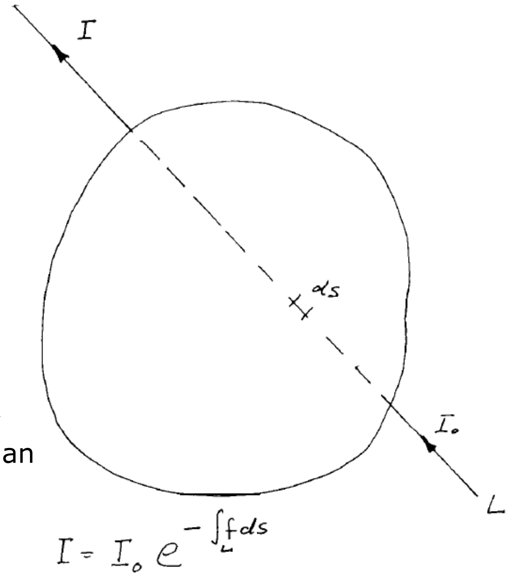

Computerized Assisted Tomography

1972: Godfrey N Hounsfiled

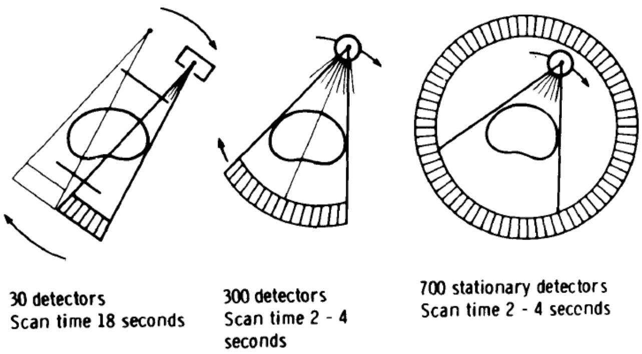

Development at EMI of X-ray computerized assisted tomography (CAT or CT scan)

Signal Processing in Tomography – INFIERI – Paris – July 15 2014

X-ray CAT or CT

1979: Hounsfield and Cormack received the Nobel Price in medicine for the development of computerized assisted tomography

Transmission tomography

$$I = I_0 \exp[-\int_{t_1}^{t_2} \mu_E(t)dt]$$

Monochromatic case

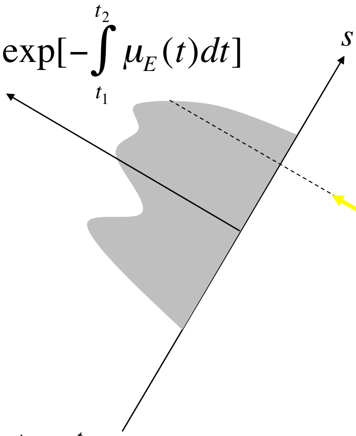

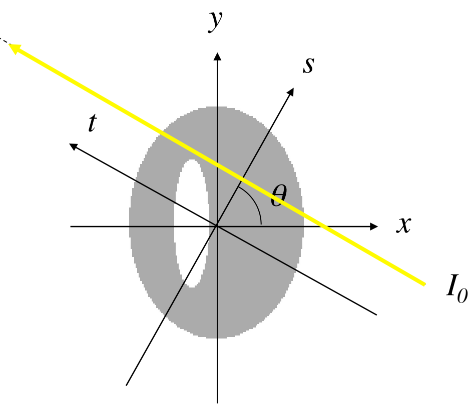

$$\ln\left(\frac{I_0}{I}\right) = \int_{t_1}^{t_2} \mu_E(t)dt$$

Transmission tomography

$$I_0 = \int_0^\infty I_0(E)\,dE$$

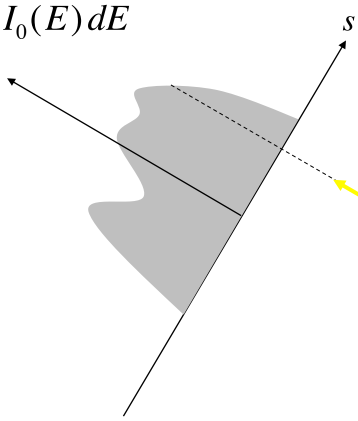

Polychromatic case

$$I = \int_0^\infty I_0(E)\exp[-\int_{t_1}^{t_2} \mu_E(t)dt]\,dE$$

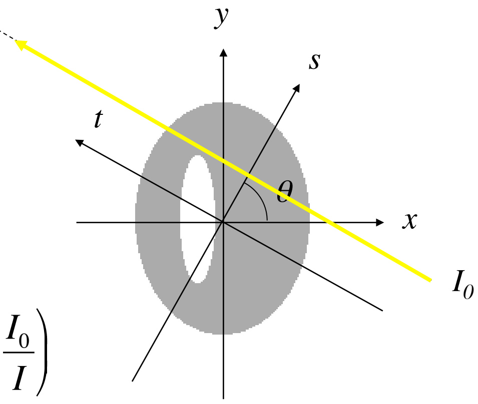

$$\ln\left(\frac{I_0(E)}{I(E)}\right) = \int_{t_1}^{t_2} \mu_E(t)dt \neq \ln\left(\frac{I_0}{I}\right)$$

Emission tomography

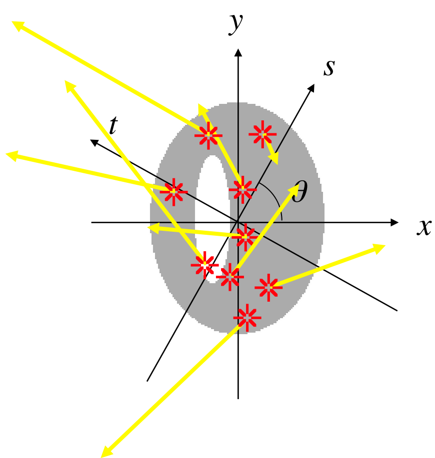

Emission tomography

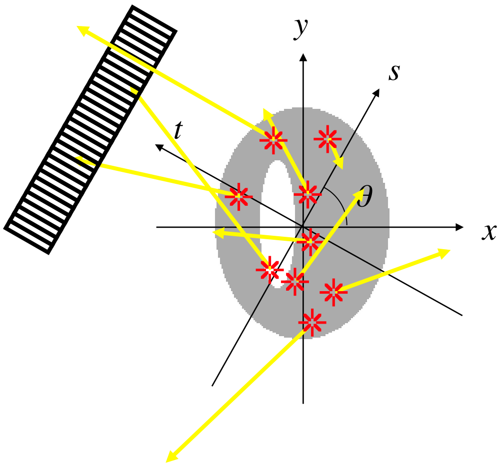

Emission tomography

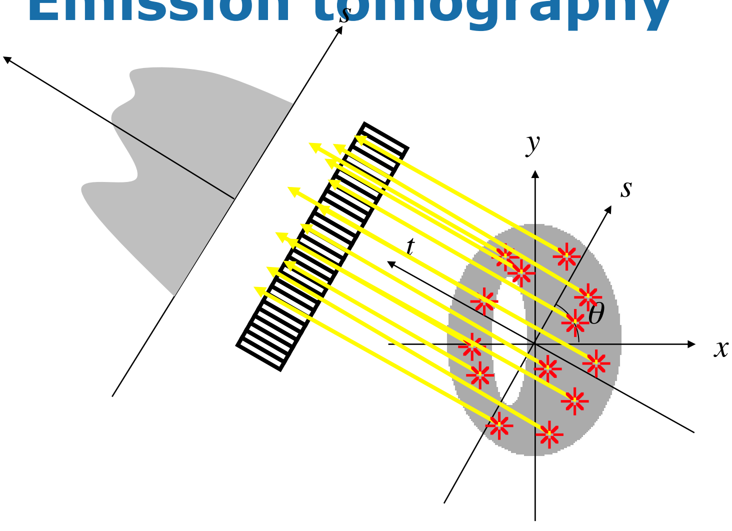

Emission tomography

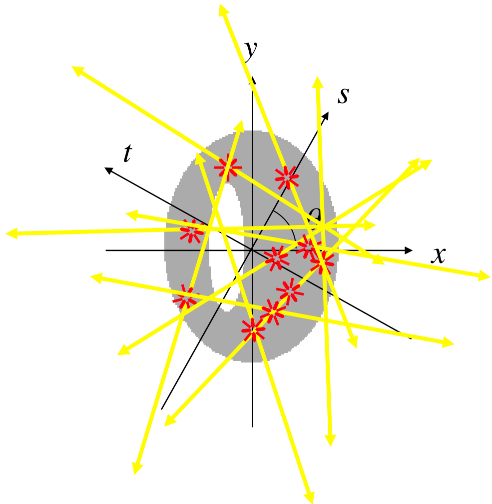

Signal Processing in Tomography – INFIERI – Paris – July 15 2014

Emission tomography

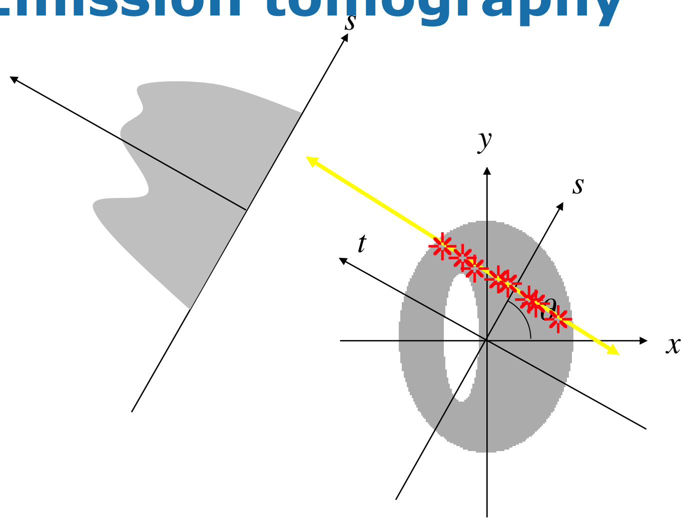

Signal Processing in Tomography – INFIERI – Paris – July 15 2014

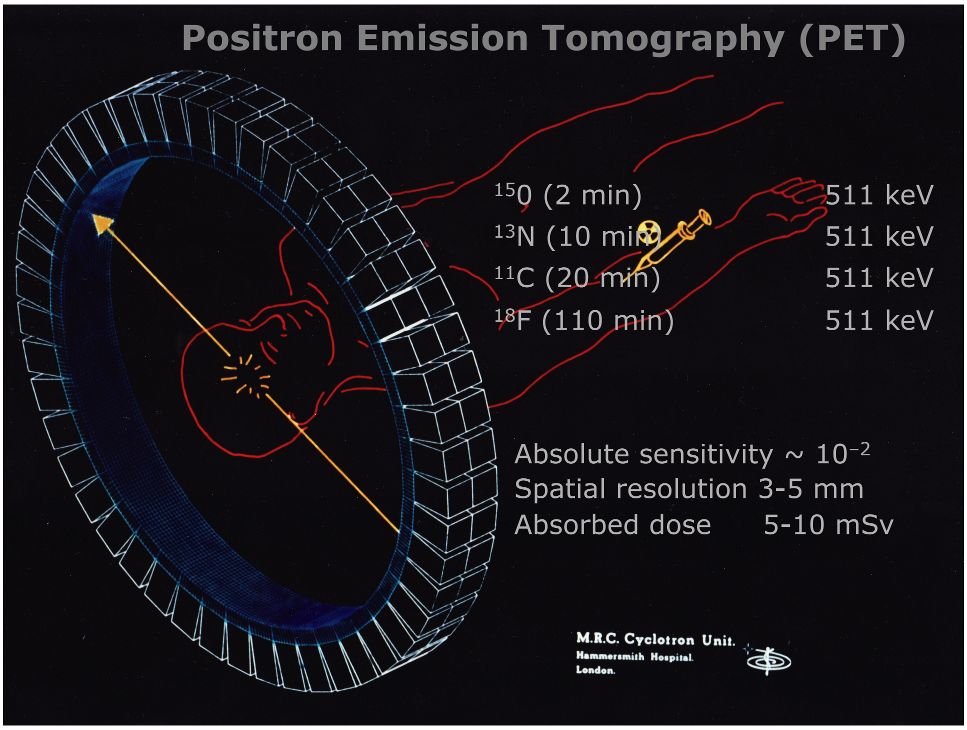

Constant progress in instrumentation

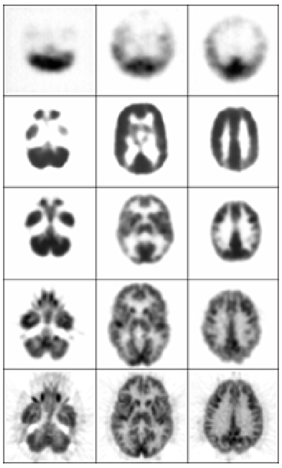

PET III 1975

ECAT II 1977

NeuroECAT 1978

ECAT 931 1985

ECAT EXACT HR+ 1995

Technical progress in PET

	BGO	LSO	GSO
Dens. [g/cm^3]	7.13	7.4	6.7
Z effectif	74	66	61
Decay [ns]	300	35-45	30-60
ph/MeV	8200	28000	10000
% NaI(Tl)	15	75	25

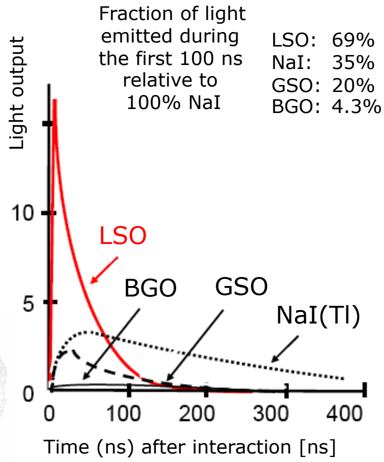

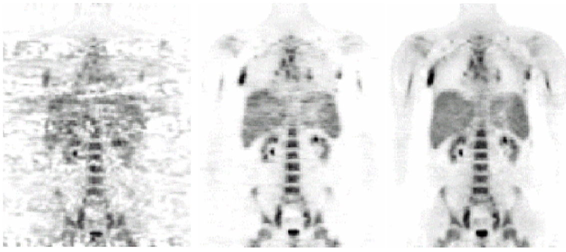

3DRP FORE+OSEM FORE+AWOSEM

courtesy: DW Townsend, UPMC

- Detectors
- Data correction
- image reconstruction

Societal application of nuclear physics

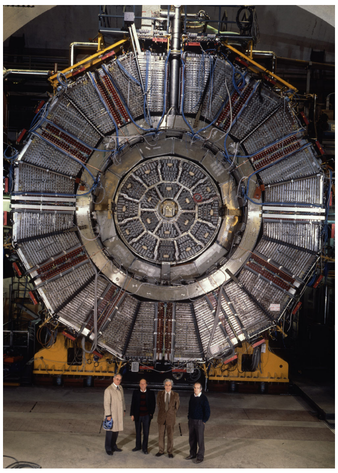

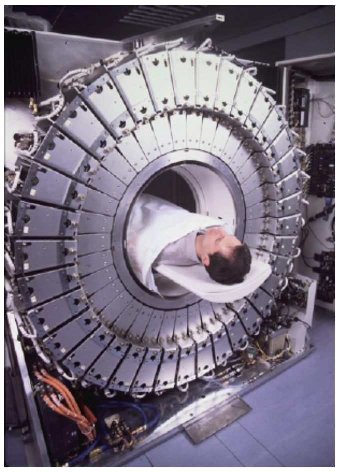

High Resolution Research Tomograph (HRRT)

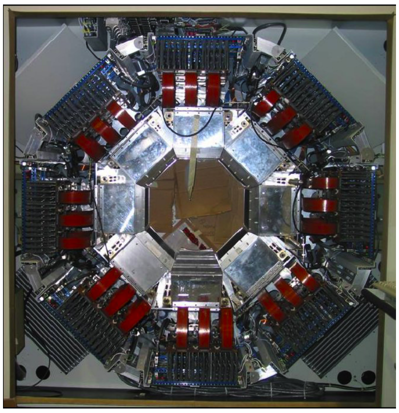

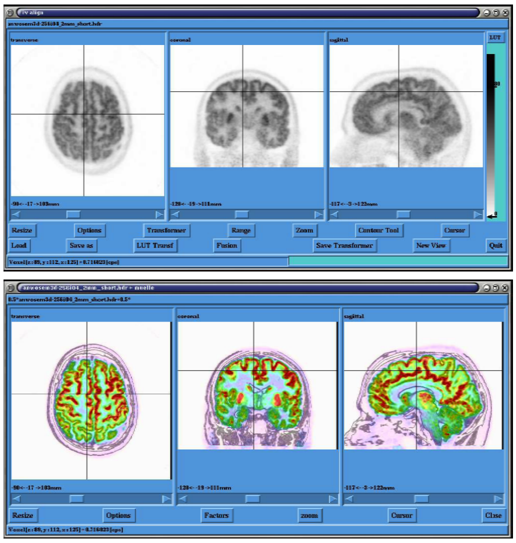

COURTESY: K.WIENHARD, KÖLN

- LSO/GSO phoswich
- 153600 crystals
- 1120 PMTs

40 min FDG fused with MRI-T1

Time-of-Flight PET (TOF-PET)

^{18}F
^{11}C
^{13}N
^{15}O

^{64}Cu
^{68}Ga
^{82}Rb

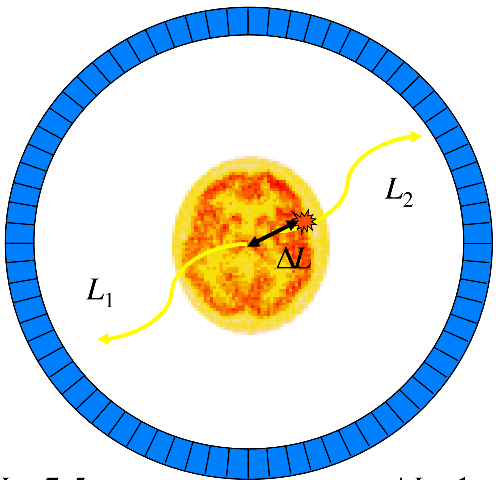

$$\Delta L = \frac{L_1 - L_2}{2}$$

$$\Delta L = \frac{1}{2} c (t_1 - t_2)$$

$$\Delta L = \frac{1}{2} c \, \Delta t$$

$\Delta t = 500\,\text{ps} \Leftrightarrow \Delta L = 7,5\,\text{cm}$

$\Delta L = 1\,\text{mm} \Leftrightarrow \Delta t = 6,7\,\text{ps}$

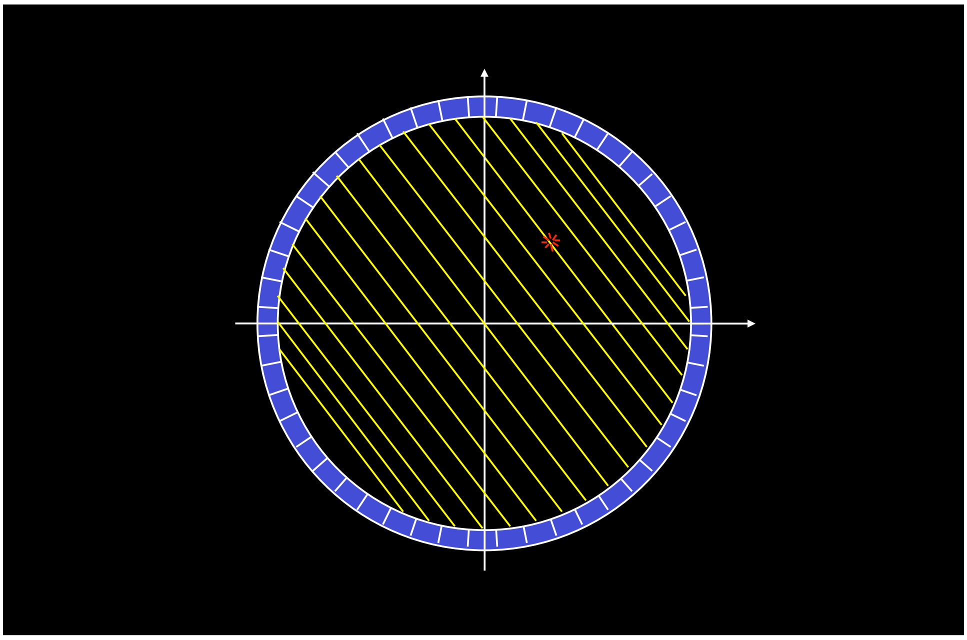

Signal Processing in Tomography – INFIERI – Paris – July 15 2014

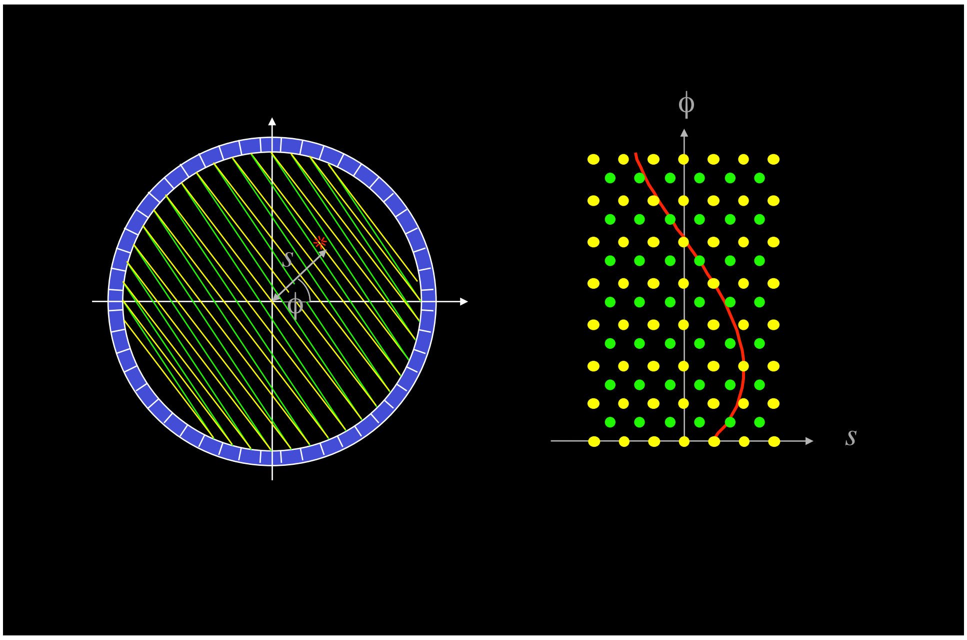

Signal Processing in Tomography – INFIERI – Paris – July 15 2014

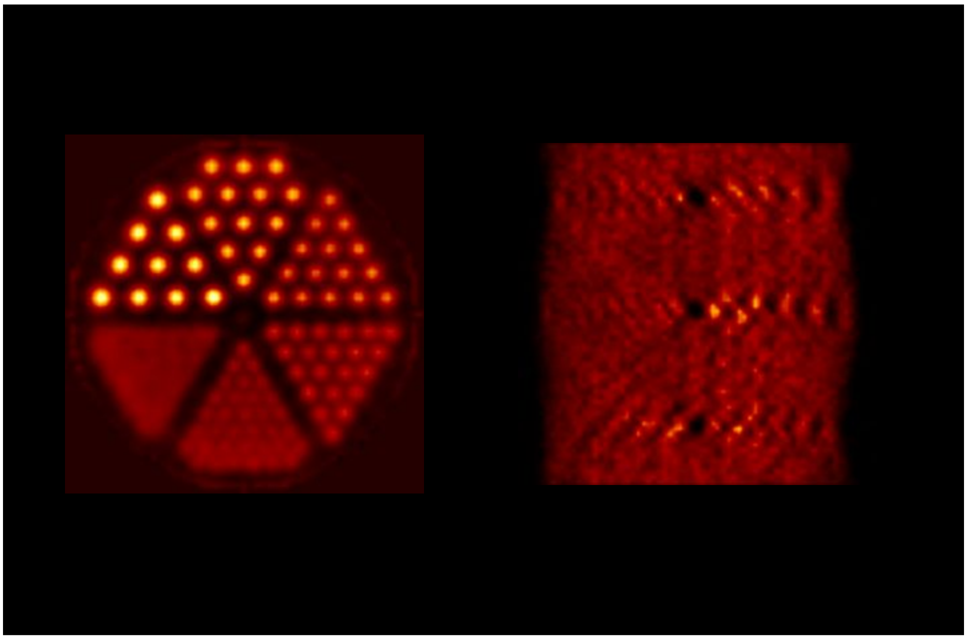

Signal Processing in Tomography – INFIERI – Paris – July 15 2014

2D PET

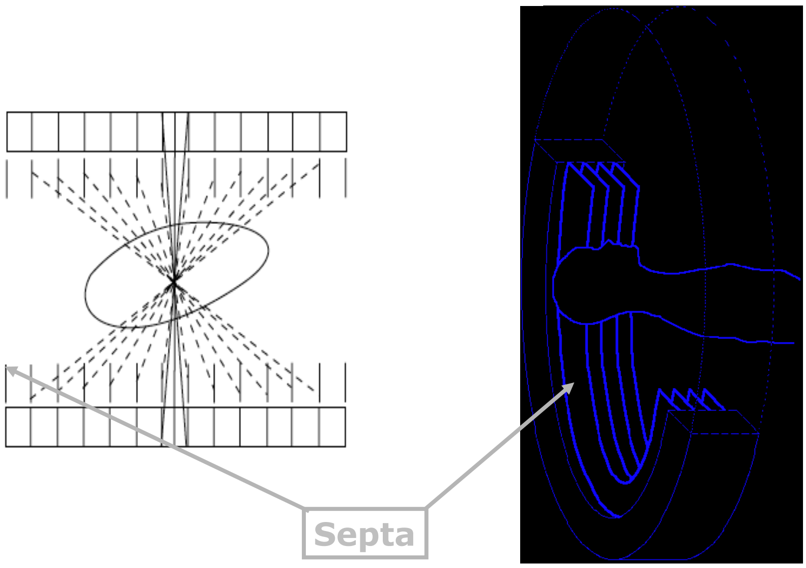

Signal Processing in Tomography – INFIERI – Paris – July 15 2014

2D …

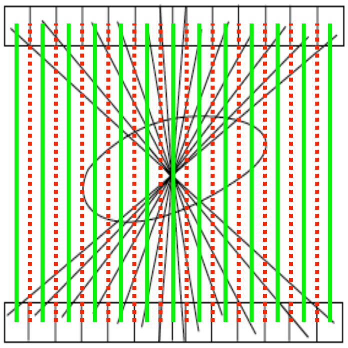

2D

3D

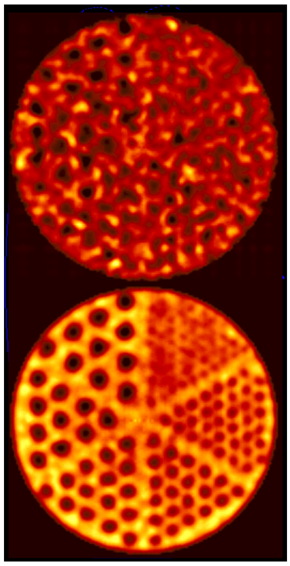

… and 3D PET

Direct LORs

Oblique LORs

n rings

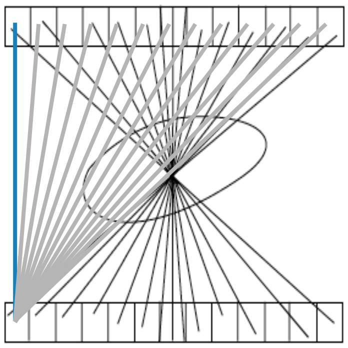

n^2 sinograms

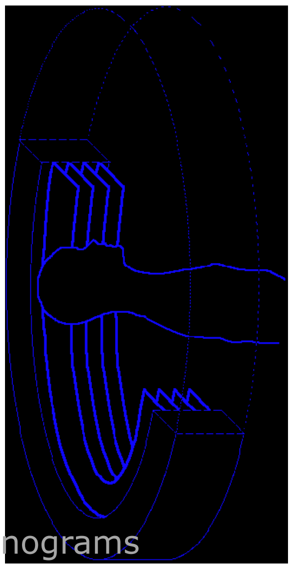

n direct sinograms

n(n−1) oblique sinograms

Signal Processing in Tomography – INFIERI – Paris – July 15 2014

… and 3D PET

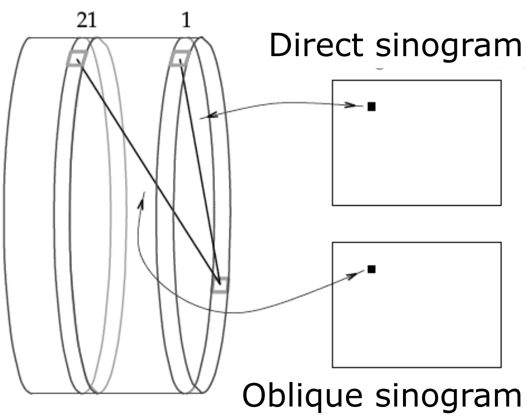

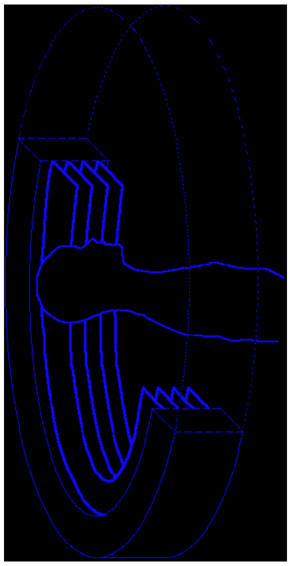

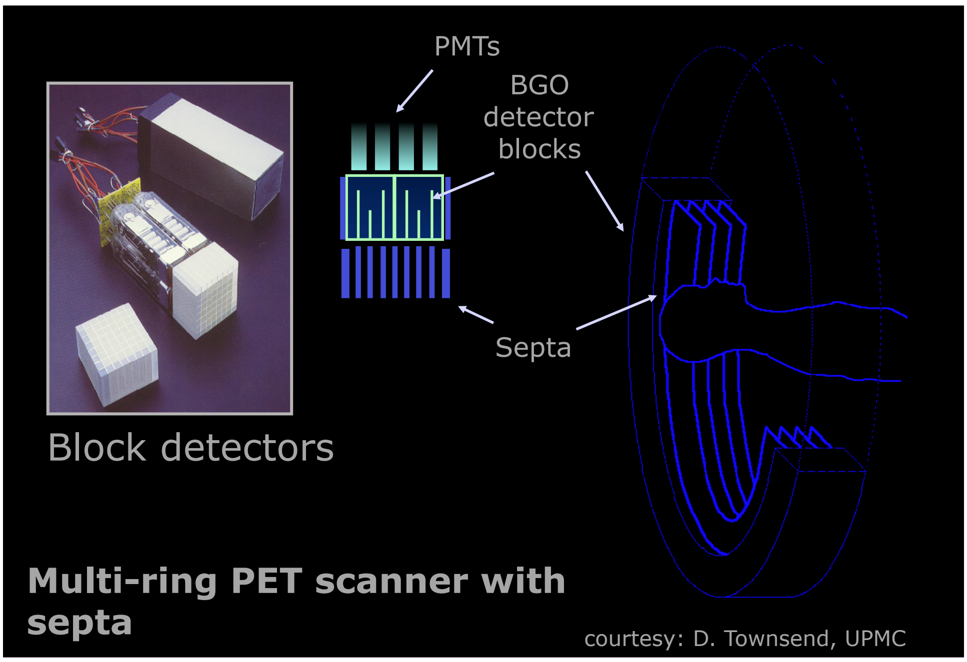

Signal Processing in Tomography – INFIERI – Paris – July 15 2014

Block detector: spatial localization

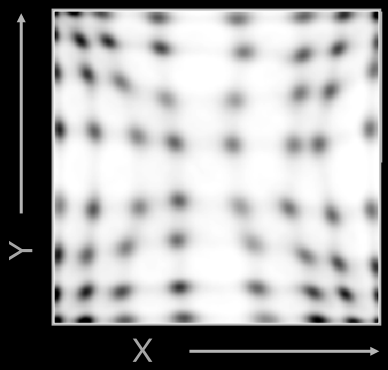

$$X = \frac{(D + B) - (C + A)}{S}$$

$$Y = \frac{(A + B) - (C + D)}{S}$$

$$S = A + B + C + D$$

where $LLD < S < ULD$

courtesy: D. Townsend, UPMC

Quadrant sharing panels

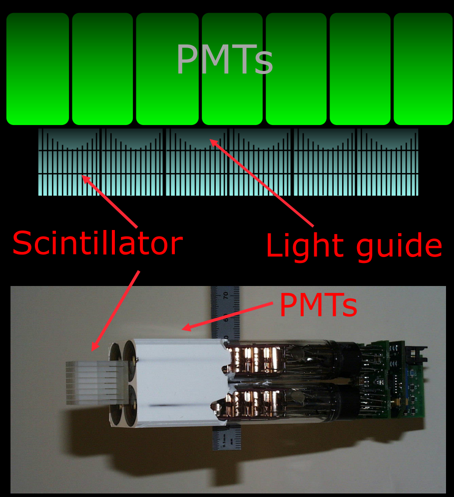

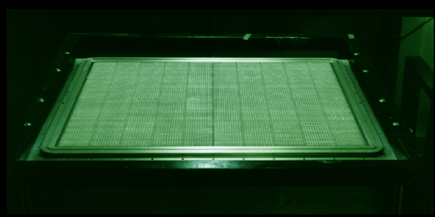

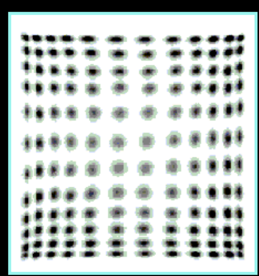

courtesy: D. Townsend, UPMC

Pixelated-continuous detector

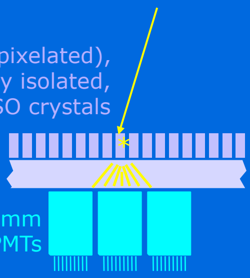

This design ensures a homogeneous response and light collection, which best preserves system energy resolution

- individual scintillating crystals
- optically continuous lightguide
- closely packed PMTs

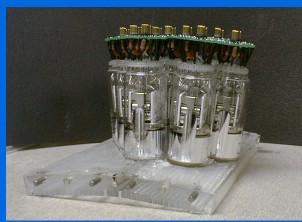

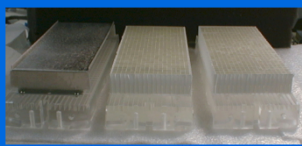

courtesy: J. Karp, U Penn

PHILIPS

Pixelated-continuous detector

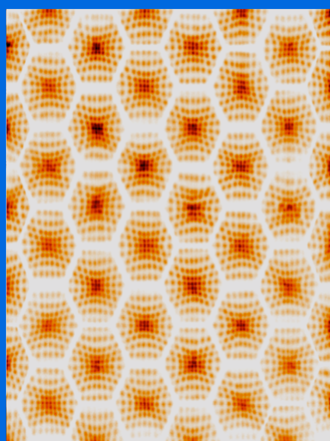

courtesy: J. Karp, U Penn

PHILIPS

Response of a rotating pair of detectors

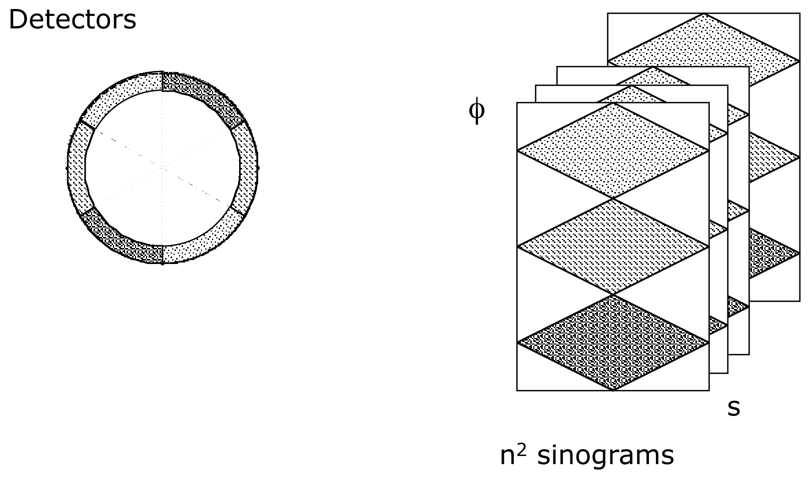

Response of a rotating pair of detectors

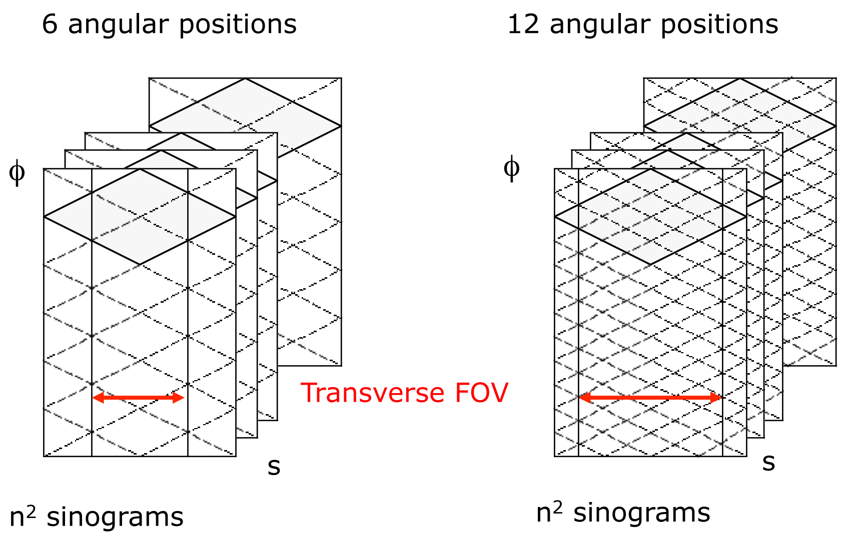

Signal Processing in Tomography – INFIERI – Paris – July 15 2014

Response from a ring of bloc detectors

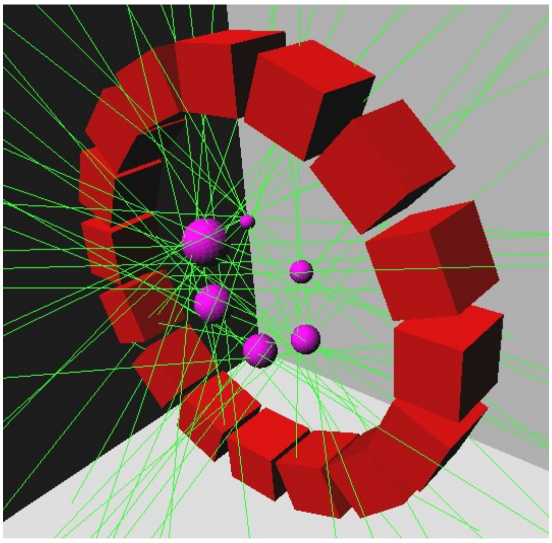

Response from a ring of bloc detectors

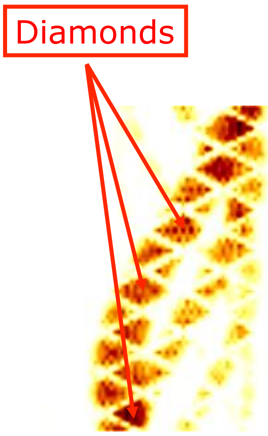

Direct sinogram

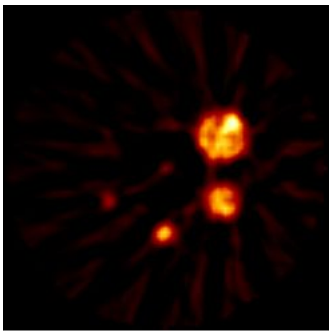

Reconstructed transverse slice

Signal Processing in Tomography – INFIERI – Paris – July 15 2014

Response from a rotating ring of bloc detectors

Direct sinogram

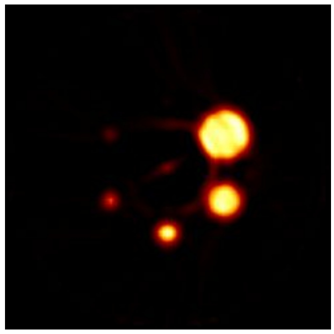

Reconstructed transverse slice

Simulation of a uniform phantom

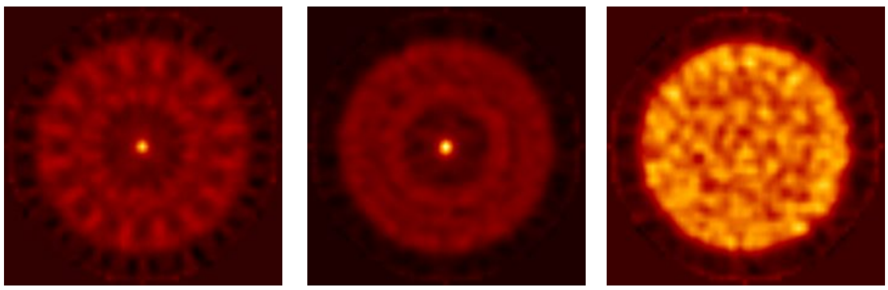

Static detectors

Rotating detectors

Not normalised

Normalised

Count rate curves in 2D and 3D PET

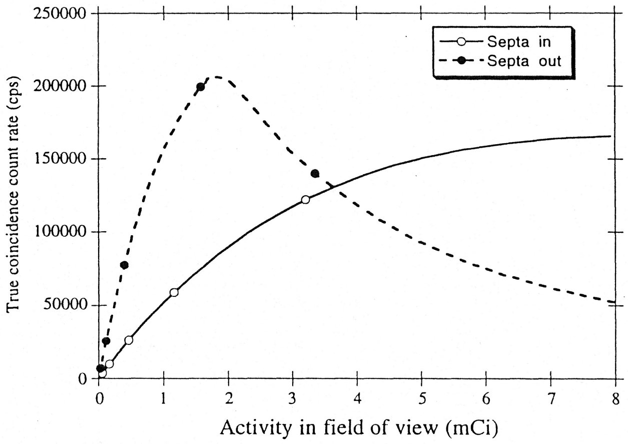

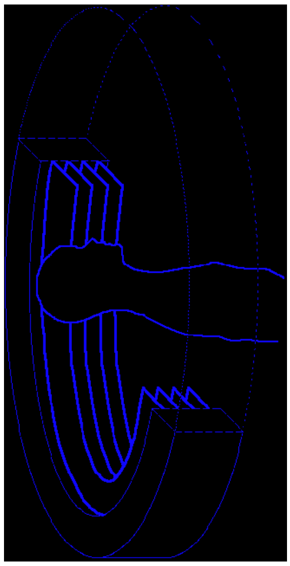

Detection of random coincidences

When N_1 gets ahead N_2

$(N_2 w) x N_1 = N_R$

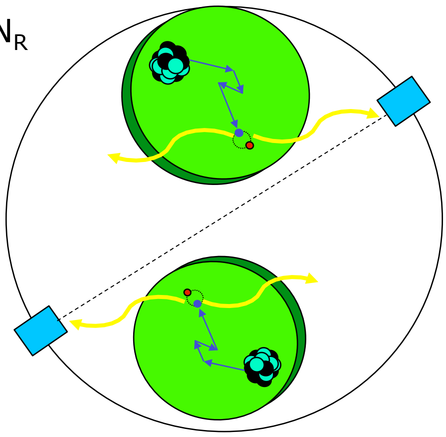

$N_1 = A \varepsilon \Omega$

$N_2 = A \varepsilon \Omega$

When N_2 gets ahead N_1

$(N_1 w) x N_2 = N_R$

Detection of random coincidences

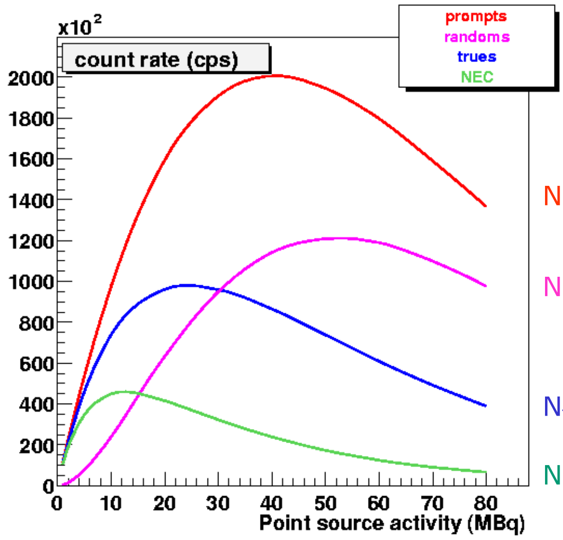

$N_{Prompts} = N_{Trues} + N_R$

$N_R = (2\ w)\ A^2\ \varepsilon^2\ \Omega^2$

$N_{Trues} = A\ \varepsilon^2\ \Omega$

$NEC = N_{Trues}^2 / (N_{Trues} + 2\ N_R)$

Detection of scattered coincidences

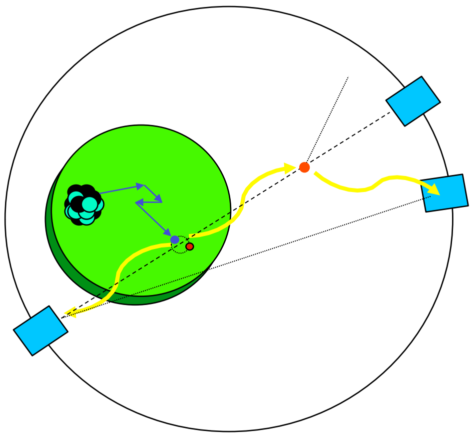

Detection of scattered coincidences

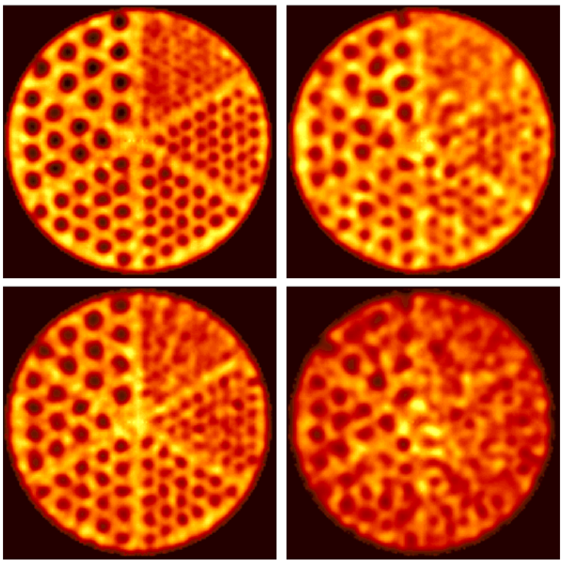

Simulation without scatter

Simulation with scatter

Central Slice Theorem

$$P_\theta(\nu_s) = F(\nu_s \cos\theta, \nu_s \sin\theta)$$

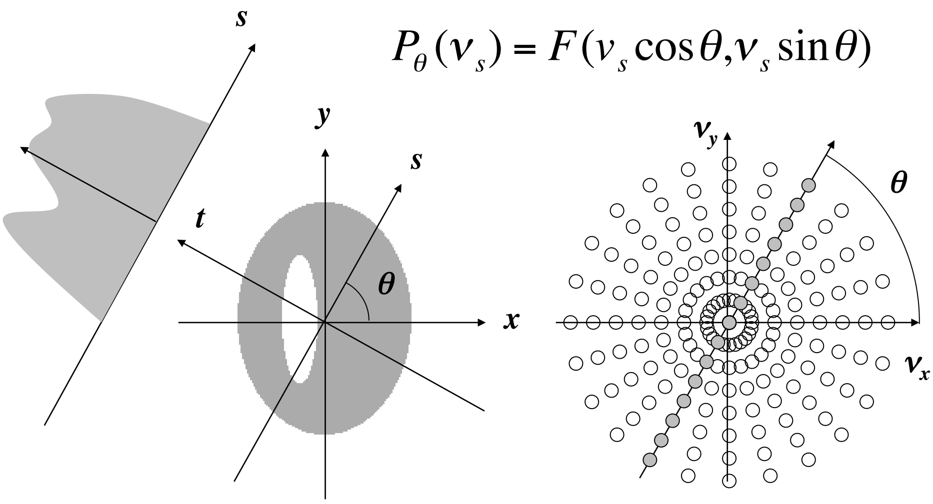

2D Filtered Back-Projection (2D FBP)

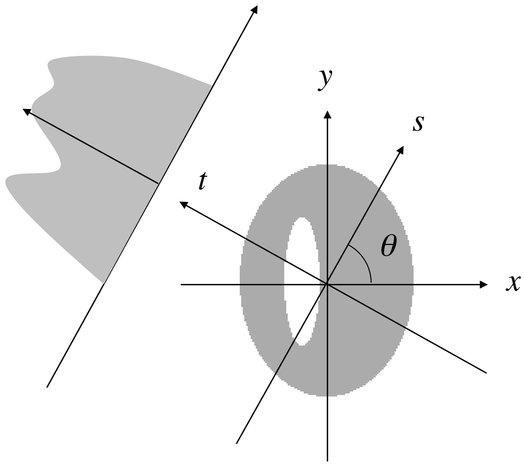

1D parallel projection

$$p_\theta(s) = \int_{-\infty}^{\infty} dt \; f(x,y)$$

Fourier Transform

$$P_\theta(\nu_s) = \int_{-\infty}^{\infty} ds \; p_\theta(s) \, e^{-i2\pi s \nu_s}$$

$$f(x,y) = \int_0^{\pi} d\theta \left[\int_{-\infty}^{\infty} d\nu_s |\nu_s| P_\theta(\nu_s) e^{i2\pi \nu_s s} \right], \quad s = x\cos\theta + y\sin\theta$$

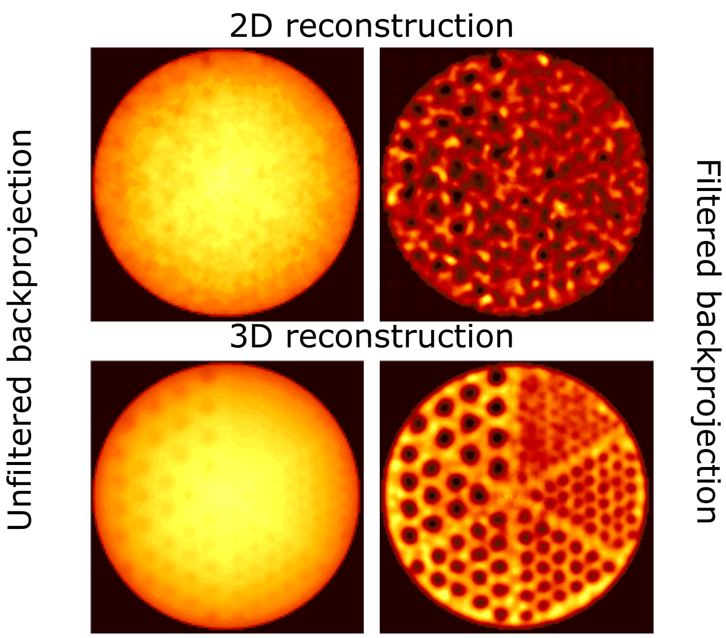

Signal Processing in Tomography – INFIERI – Paris – July 15 2014

Image reconstruction

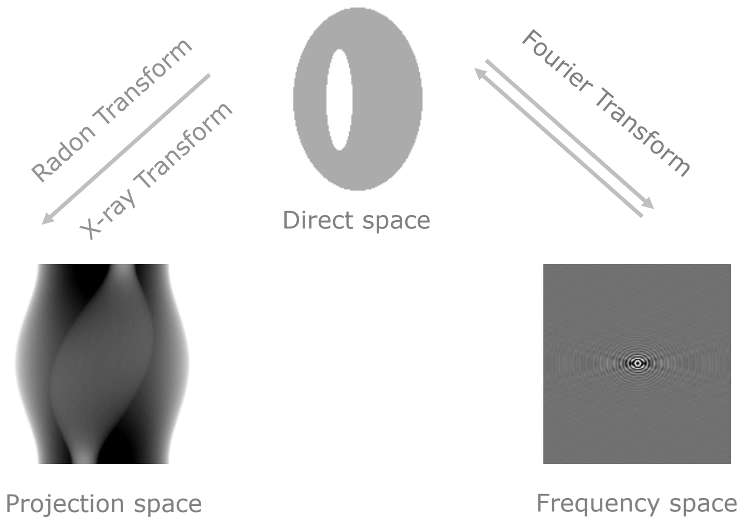

Inversion of the 3D Radon Transform

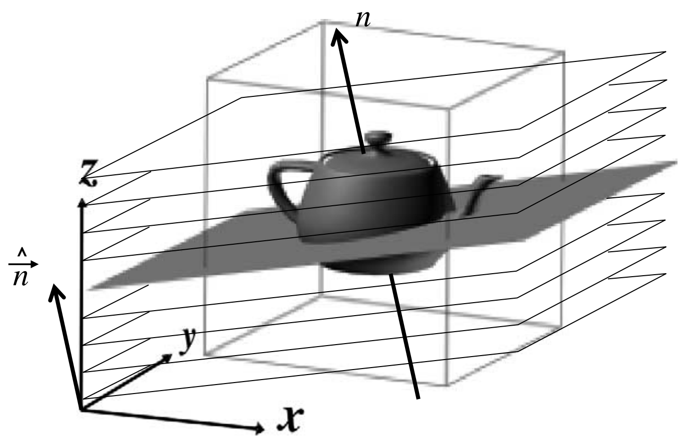

Modulation Transfer Function of a 2D Filter

$$T(\vec{v}_{3D}) = \iint_{\Omega} \mathrm{d}^2\hat{u}\; \delta(\hat{\hat{u}}\cdot \vec{v}_{3D})\; H(\hat{\hat{u}},\vec{v}_{3D}) = 1, \forall\, \vec{v}_{3D} \in \mathrm{R}^{3*}$$

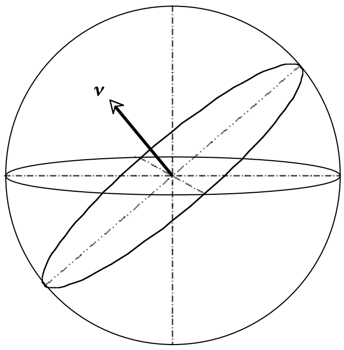

$$T(\vec{v}_{3D}) = \iint_{4\pi} \mathrm{d}^2\hat{u} \frac{1}{\|\vec{v}_{3D}\|} \delta(\hat{\hat{u}}\cdot \frac{\vec{v}_{3D}}{\|\vec{v}_{3D}\|}) = \frac{2\pi}{\|\vec{v}_{3D}\|}$$

2D Colsher Filter (1980)

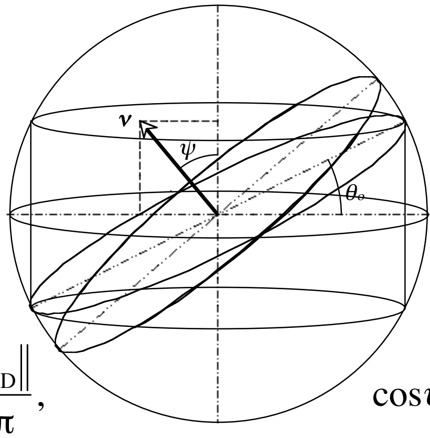

$$H_{Colsher}\left(\vec{v}_{3D}\right) = \begin{cases} \dfrac{\|\vec{v}_{3D}\|}{2\pi}, & \cos\psi \geq \cos\theta_0 \\ \dfrac{\|\vec{v}_{3D}\|}{4} \dfrac{1}{\arcsin(\sin\theta_0 / \sin\psi)}, & \cos\psi < \cos\theta_0 \end{cases}$$

Signal Processing in Tomography – INFIERI – Paris – July 15 2014

3D Re-Projection algorithm (3DRP)

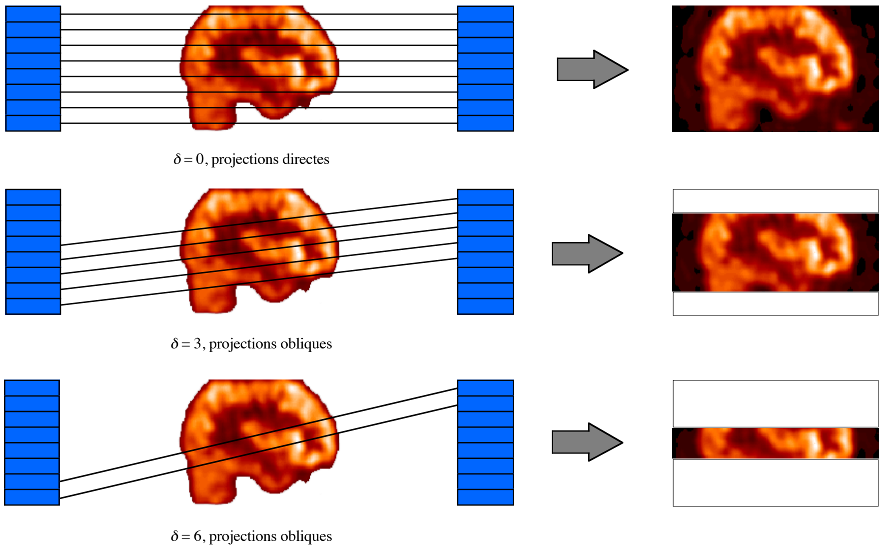

Signal Processing in Tomography – INFIERI – Paris – July 15 2014

3D Re-Projection algorithm (3DRP)

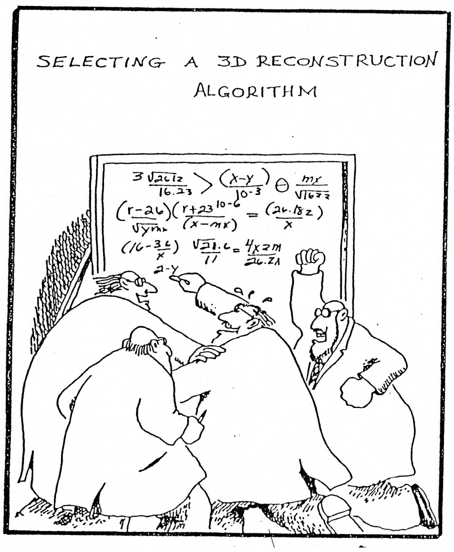

Signal Processing in Tomography – INFIERI – Paris – July 15 2014

Image reconstruction and statistics

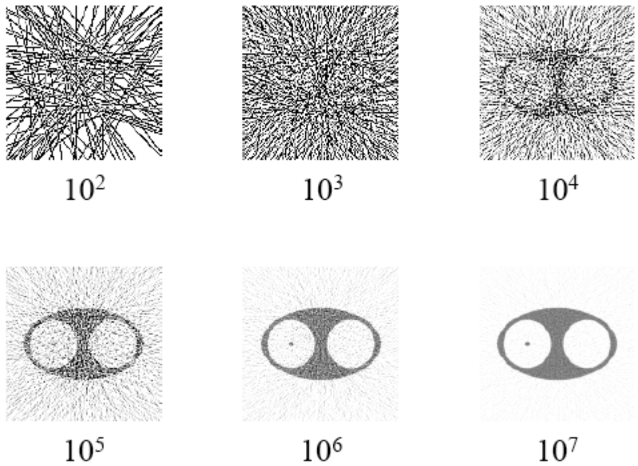

courtesy: C. Comtat, CEA-SHFJ

Signal-to-noise ratio and counting statistics

$$\frac{A}{\Delta A} = \sqrt{N_{\beta^+}} \Rightarrow N_{\beta^+} = \left(\frac{A}{\Delta A}\right)^2$$

$$N_{Tot} = \left(\frac{L}{d}\right)^3 \times \left(\frac{A}{\Delta A}\right)^2 \times \left(\frac{L}{d}\right)$$

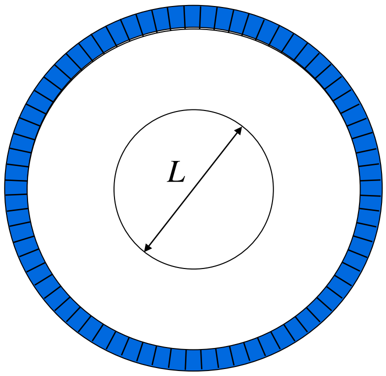

Improving spatial resolution by a factor 2 involves to increase statistics by a factor 16 to getting the same signal-to-noise ratio in the reconstructed image

Signal-to-noise ratio and counting statistics

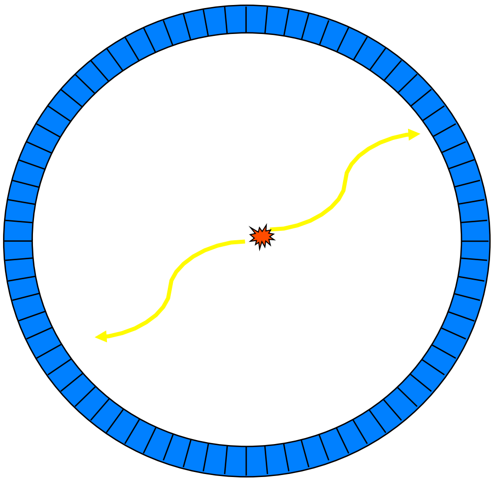

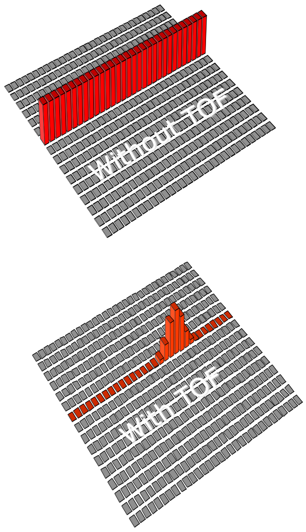

TOF-PET and improvement of SNR

$$N_{Tot} = \left(\frac{L}{d}\right)^3 \times \left(\frac{A}{\Delta A}\right)^2 \times \left(\frac{L}{d}\right)$$

$$N_{ToF} = \left(\frac{L}{d}\right)^3 \times \left(\frac{A}{\Delta A}\right)^2 \times \left(\frac{\Delta L}{d}\right)$$

Variance reduction factor $f = \frac{L}{\Delta L} = \frac{2L}{c\Delta t}$

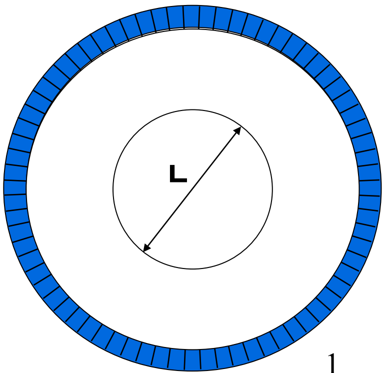

$\Delta L = \frac{1}{2} c\, \Delta t$

$$\text{Whole-body imaging L = 35 cm} \Rightarrow f > 1 \text{ if } \Delta t < 2{,}3 \text{ ns}$$

$$\text{Brain imaging L = 20 cm} \Rightarrow f > 1 \text{ if } \Delta t < 1{,}3 \text{ ns}$$

Signal Processing in Tomography – INFIERI – Paris – July 15 2014

Support of the Fourier Transform of the X-ray Transform

$$g(s,\phi) = \int dt\, f(s\cos\phi - t\sin\phi, s\sin\phi + t\cos\phi)$$

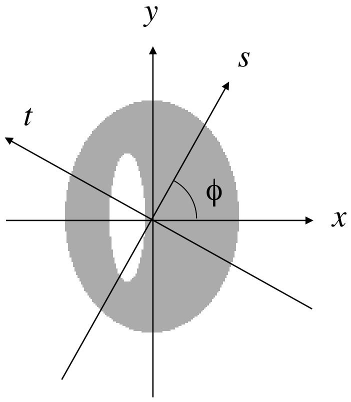

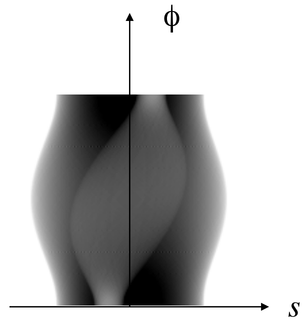

Support of the Fourier Transform of the X-ray Transform

$$G(\nu_s,\kappa_\phi) = \mathrm{TF}_{2D}[g(s,\phi)]$$

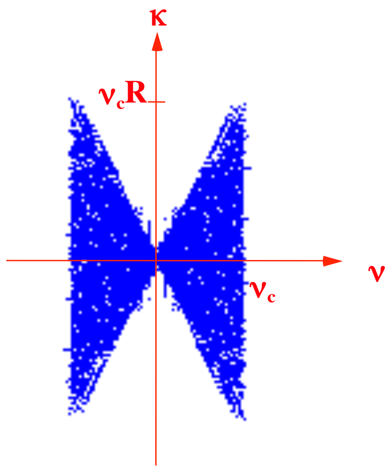

$$g(s,\phi) = \int dt\, f(s\cos\phi - t\sin\phi, s\sin\phi + t\cos\phi)$$

Orthogonal sampling of the 2D X-ray Transform

Fourier space

$$(W^{-1})^T = \begin{pmatrix} 2\nu_c & 0 \\ 0 & 2\nu_c R \end{pmatrix}$$

Direct Space

$$W = \begin{pmatrix} \frac{1}{2\nu_c} & 0 \\ 0 & \frac{1}{2\nu_c R} \end{pmatrix}$$

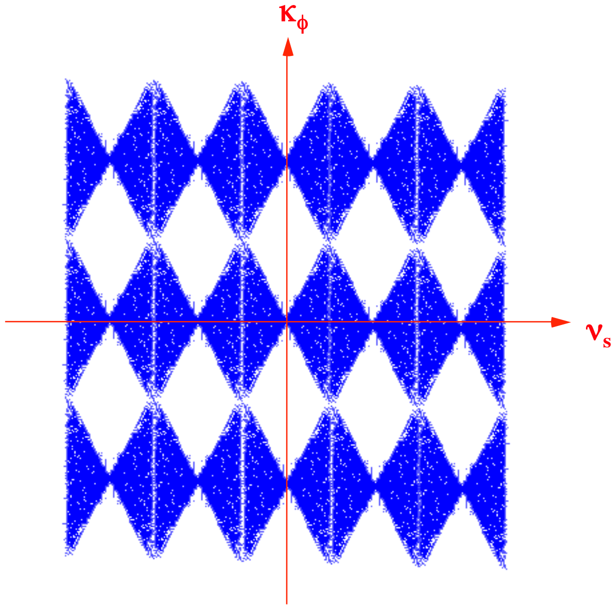

Interleaved sampling of the 2D X-ray Transform

Fourier Space

$$(W^{-1})^T = \begin{pmatrix} 2\nu_c & \nu_c \\ 0 & \nu_c R \end{pmatrix}$$

Direct space

$$W = \begin{pmatrix} \frac{1}{2\nu_c} & 0 \\ -\frac{1}{2\nu_c R} & \frac{1}{\nu_c R} \end{pmatrix}$$

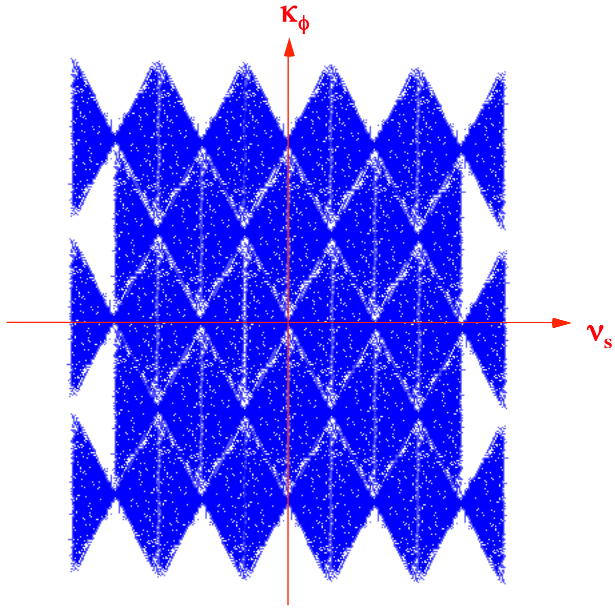

Signal Processing in Tomography – INFIERI – Paris – July 15 2014

Support of the Fourier Transform of the 3D transverse X-ray Transform

$$G(\nu_s, \kappa_\phi, \tau_z) = \mathrm{TF}_{3\mathrm{D}}[g(s, \phi, z)]$$